

Cite this: *Chem. Sci.*, 2015, **6**, 5690

Carbon nitride– TiO_2 hybrid modified with hydrogenase for visible light driven hydrogen production†

Christine A. Caputo,^a Lidong Wang,^b Radim Beranek^b and Erwin Reisner^{*a}

A system consisting of a [NiFeSe]–hydrogenase (H₂ase) grafted on the surface of a TiO₂ nanoparticle modified with polyheptazine carbon nitride polymer, melon (CN_x) is reported. This semi-biological assembly shows a turnover number (TON) of more than 5.8×10^5 mol H₂ (mol H₂ase)^{−1} after 72 h in a sacrificial electron donor solution at pH 6 during solar AM 1.5 G irradiation. An external quantum efficiency up to 4.8% for photon-to-hydrogen conversion was achieved under irradiation with monochromatic light. The CN_x–TiO₂–H₂ase construct was also active under UV-free solar light irradiation ($\lambda > 420$ nm), where it showed a substantially higher activity than TiO₂–H₂ase and CN_x–H₂ase due, in part, to the formation of a CN_x–TiO₂ charge transfer complex and highly productive electron transfer to the H₂ase. The CN_x–TiO₂–H₂ase system sets a new benchmark for photocatalytic H₂ production with a H₂ase immobilised on a noble- and toxic-metal free light absorber in terms of visible light utilisation and stability.

Received 5th June 2015

Accepted 29th June 2015

DOI: 10.1039/c5sc02017d

www.rsc.org/chemicalscience

Introduction

The use of efficient electrocatalysts in artificial photocatalytic schemes has been an area of recent interest for the conversion of protons to hydrogen using sunlight. Specifically, the use of redox enzymes in photocatalytic schemes highlights the importance of investigating the compatibility of biological systems with light harvesting materials and testing the stability of the resultant bio-hybrid assemblies.¹ Hydrogenases (H₂ases) are the most efficient noble-metal free electrocatalysts for H₂ production and achieve a turnover frequency (TOF) of more than 1000 s^{−1} with a small overpotential.² H₂ases also show impressive H₂ production rates and yields in sacrificial photocatalytic schemes in pH neutral aqueous solution.^{3a} In these systems, a photoexcited light absorber provides electrons to the protein *via* an internal wire, the iron–sulfur electron relay, to the active site where proton reduction occurs. Examples are the immobilization of a H₂ase on Ru-sensitised TiO₂,³ on Cd-based quantum dots⁴ as well as homogeneous systems using the H₂ase with a covalently linked photosystem I⁵ or in combination with an organic dye,⁶ and multi-component systems with a dye and a soluble redox mediator.⁷

Polymeric carbon nitride (polyheptazine or melon, herein CN_x) is a promising visible-light absorber for the photocatalytic generation of H₂.⁸ We have recently reported the use of CN_x as a light harvesting material in combination with a H₂ase and a H₂ase-inspired synthetic Ni catalyst for solar H₂ generation.⁹ The CN_x–H₂ase system showed sustained catalysis with a turnover number (TON) of more than 50 000 after 70 h solar light irradiation. However, this hybrid system suffered from a weak interaction between the H₂ase and the CN_x surface, and consequently, poor electron transfer from CN_x to the H₂ase. Furthermore, CN_x–H₂ase only showed efficient H₂ production up to wavelengths of approximately 420 nm and therefore only limited visible light harvesting capabilities.

Here, we selected a hybrid material consisting of TiO₂ (Hombikat UV 100, anatase, BET surface area: 300 m² g^{−1}, crystallite size < 10 nm) surface-modified with CN_x polymer as a light absorbing hybrid material for the photocatalytic system with a H₂ase for three main reasons (Fig. 1; see ESI and Fig. S1† for synthesis and characterisation). Firstly, CN_x–TiO₂ can be readily prepared on a gram scale by heating TiO₂ nanoparticles in the presence of urea, an inexpensive and sustainable material.¹⁰

Secondly, CN_x–TiO₂ provides us with substantially improved solar light harvesting performance compared to individual CN_x and TiO₂. *Band gap excitation* of TiO₂ (pathway 1; Fig. 1) efficiently utilises the UV spectrum (band gap of 3.2 eV for anatase TiO₂ with CB_{TiO₂} at approximately −0.6 V vs. NHE at pH 6).¹¹ A significant portion of the visible spectrum is utilised with CN_x–TiO₂ as it can, upon photo-excitation of CN_x, perform *photoinduced electron transfer* from the LUMO_{CN_x} to CB_{TiO₂} (pathway 2).

^aChristian Doppler Laboratory for Sustainable SynGas Chemistry, Department of Chemistry, Cambridge University, Lensfield Road, Cambridge CB2 1EW, UK. E-mail: reisner@ch.cam.ac.uk; Web: <http://www-reisner.ch.cam.ac.uk>

^bFaculty of Chemistry and Biochemistry, Ruhr-Universität Bochum, Universitätsstraße 150, 44780 Bochum, Germany

† Electronic supplementary information (ESI) available. See DOI: [10.1039/c5sc02017d](https://doi.org/10.1039/c5sc02017d)



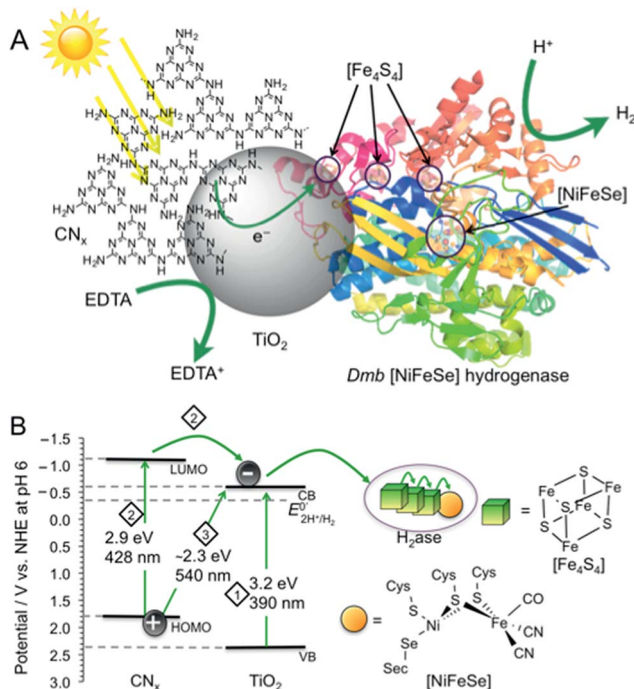


Fig. 1 (A) Schematic representation of photo-H₂ production with *Dmb* [NiFeSe]–H₂ase (PDB ID : 1CC1)¹⁴ on CN_x–TiO₂ suspended in water containing EDTA as a hole scavenger. (B) Irradiation of CN_x–TiO₂ can result in photo-induced electron transfer by three distinct pathways: (1) TiO₂ band gap excitation (2) excitation of CN_x (HOMO_{CNx}–LUMO_{CNx}), followed by electron transfer from LUMO_{CNx} into the conduction band of TiO₂ (CB_{TiO₂}). (3) Charge transfer excitation with direct optical electron transfer from HOMO_{CNx} to CB_{TiO₂}. The CB_{TiO₂} electrons generated through pathways 1 to 3 are then transferred via the [Fe₄S₄] clusters to the [NiFeSe] H₂ase active site.

In addition, *direct optical electron transfer* can occur from the HOMO_{CNx} (with contributions of molecular orbitals formed upon interaction of CN_x with TiO₂)¹² directly to the CB_{TiO₂} (pathway 3), extending the absorption even further into the visible region (up to 540 nm). This absorption pathway 3 is based on strong coupling between CN_x covalently grafted onto TiO₂, resulting in strong charge-transfer absorption. Conclusive evidence of this charge-transfer includes previously reported spectroscopic, photoelectrochemical, and theoretical investigations.^{12,13} The generated CB_{TiO₂} electrons provide the H₂ase with an overpotential of approximately 0.2 V for proton reduction.

Thirdly, the H₂ evolution catalyst employed in this study, *Desulfomicrobium baculum* (*Dmb*) [NiFeSe]–hydrogenase is not only known for its high H₂ evolution activity, lack of H₂ inhibition and O₂-tolerance,^{6,14b,14c,15} but also for its *titaniaphilicity*.^{3a} This high affinity of the enzyme to adsorb strongly to TiO₂ stems presumably from a protein surface rich in glutamic and aspartic acid residues close to the distal [Fe₄S₄] cluster, which act as anchor sites to TiO₂ and allow for stable binding and efficient electron flow into the hydrogenase active site (Fig. 1A).^{1a,3a} Thus, the CN_x–TiO₂ hybrid is expected to support a more robust H₂ase-particle interaction than with CN_x alone,

which would result in improved charge transfer and ultimately increased catalytic turnover for H₂ production.

Results and Discussion

Photocatalytic systems were assembled by dispersing CN_x–TiO₂ particles in an aqueous electron donor solution (0.1 M; 2.98 mL) in a photoreactor vessel (headspace volume: 4.74 mL; see ESI[†] for experimental details). The vessel was sonicated under air (15 min) before sealing and purging with an inert gas (2% CH₄ in N₂). The H₂ase (16.5 μ L, 3 μ M) was then added and the photoreactor purged again to ensure anaerobic conditions. The stirred suspension was irradiated at 25 °C with a solar light simulator (air mass 1.5 global filter, $I = 100$ mW cm⁻²) and the headspace H₂ was quantified at regular time intervals by gas chromatography against the internal CH₄ standard. The conditions were optimised for maximum turnover frequency (TOF_{H₂ase}) by varying the electron donor and pH of the solution (Table S1; Fig. S2 and S3[†]). Optimised conditions consisted of ethylenediamine tetraacetic acid (EDTA; 0.1 M) as the electron donor at pH 6. A ratio of semiconductor (5 mg unless otherwise noted) to H₂ase (50 pmol) was used for ease of comparison to previously reported photosystems with *Dmb* [NiFeSe]–H₂ase.^{3,6,9}

Solar (UV-visible) irradiation ($\lambda > 300$ nm) of CN_x–TiO₂–H₂ase under standard conditions generated an initial TOF_{H₂ase} of $(2.8 \pm 0.3) \times 10^4$ h⁻¹ or 8 s⁻¹ with the production of 5.85 ± 0.59 μ mol H₂ after 4 h and 28 ± 3 μ mol H₂ with an overall TON_{H₂ase} $> (5.8 \pm 0.6) \times 10^5$ after 72 h (Fig. 2 and S4[†]). Negligible amounts of H₂ were detected in the absence of H₂ase, CN_x–TiO₂ or EDTA. UV band gap excitation of TiO₂ did not result in the accumulation of O₂, which suggests that holes generated upon UV band gap excitation of TiO₂ are either efficiently quenched by EDTA directly or scavenged after being trapped by CN_x.

To qualitatively determine the contributions from the three excitation pathways in Fig. 1B, irradiation was also performed with different long-pass filters. The CN_x–TiO₂–H₂ase system was studied under visible light irradiation at $\lambda > 420$ nm to study the contribution of CN_x to light absorption (pathways 2 & 3) without

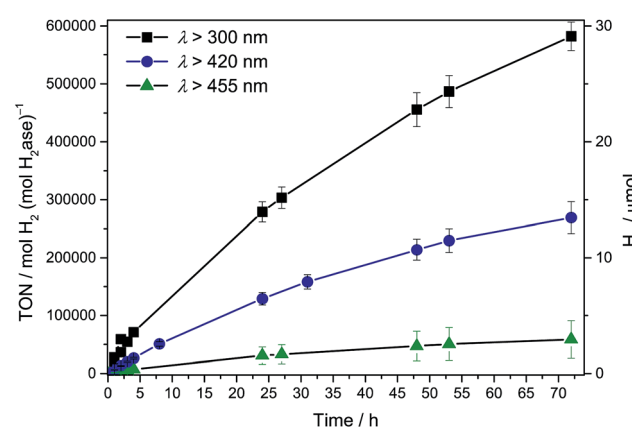


Fig. 2 Photocatalytic H₂ production with *Dmb* [NiFeSe]–H₂ase (50 pmol) with CN_x–TiO₂ (5 mg) in EDTA (pH 6, 0.1 M, 3 mL) under AM 1.5G irradiation at an intensity of 1 Sun at $\lambda > 300$, 420 and 455 nm.

the contribution of intrinsic absorption by TiO_2 (pathway 1). A photoactivity with an initial $\text{TOF}_{\text{H}_2\text{ase}}$ of $6353 \pm 635 \text{ h}^{-1}$ was observed, which results in the generation of $1.31 \pm 0.13 \mu\text{mol H}_2$ after 4 h. After 72 h, $13 \pm 1 \mu\text{mol}$ of H_2 were generated with a $\text{TON}_{\text{H}_2\text{ase}}$ of more than $(2.6 \pm 0.3) \times 10^5$ (Fig. 2).

Subsequently, irradiation was carried out at $\lambda > 455 \text{ nm}$ to investigate the contribution of the direct charge-transfer from the $\text{HOMO}_{\text{CN}_x}$ to CB_{TiO_2} to the photoactivity. A $\text{TOF}_{\text{H}_2\text{ase}}$ of $1096 \pm 175 \text{ h}^{-1}$ with the evolution of $0.26 \pm 0.06 \mu\text{mol H}_2$ after 4 h and $2.9 \pm 1.6 \mu\text{mol H}_2$ after 72 h was observed, which corresponds to 17% of the visible light activity. This suggests that all three pathways in Fig. 1B contribute to the UV-vis photoactivity, whereas pathways 2 and 3 are responsible for the visible-light response of $\text{CN}_x\text{-TiO}_2\text{-H}_2\text{ase}$. Previous investigations of $\text{CN}_x\text{-TiO}_2$ hybrids have shown that their activity is limited by the strong electronic coupling between CN_x and TiO_2 leading not only to intense visible light absorption but also to fast back electron transfer (primary recombination).^{13,16}

In order to study the role of TiO_2 as heterogeneous electron relay in $\text{CN}_x\text{-TiO}_2\text{-H}_2\text{ase}$ in more detail, a sample of $\text{CN}_x\text{-ZrO}_2$ (15 mg) was also tested with the H_2ase . The negative CB_{ZrO_2} at approximately -1.35 V vs. NHE at pH 6, prevents electron injection from $\text{LUMO}_{\text{CN}_x}$ (approximately -1.25 V vs. NHE at pH 6).¹⁷ This band level mismatch allowed us to demonstrate that spatial proximity of surface-bound H_2ase to CN_x alone cannot promote productive electron transfer as no H_2 was observed with $\text{CN}_x\text{-ZrO}_2\text{-H}_2\text{ase}$ ($\lambda > 300 \text{ nm}$; Fig. S4†). Thus, charge transfer from the $\text{LUMO}_{\text{CN}_x}$ into CB_{ZrO_2} (pathway 2) is not possible, nor is the direct electron transfer from $\text{HOMO}_{\text{CN}_x}$ to CB_{ZrO_2} (pathway 3), which are crucial to the formation of H_2 with the hybrid material.

For comparison, H_2 production was also tested with CN_x (5 mg) and H_2ase (50 pmol) in the absence of metal oxide under standard conditions. A $\text{TON}_{\text{H}_2\text{ase}}$ of 14852 ± 1485 was obtained after 4 h with an initial TOF of $6288 \pm 649 \text{ h}^{-1}$ when irradiated with UV-visible light ($\lambda > 300 \text{ nm}$, Table S1†). Under visible light irradiation ($\lambda > 420 \text{ nm}$), a $\text{TON}_{\text{H}_2\text{ase}}$ of 2375 ± 267 was observed after 4 h and no H_2 was produced at $\lambda > 455 \text{ nm}$, demonstrating the substantially enhanced activity with $\text{CN}_x\text{-TiO}_2\text{-H}_2\text{ase}$ compared to $\text{CN}_x\text{-H}_2\text{ase}$ at all wavelengths (Fig. S4†).

Experiments were also performed with $\text{TiO}_2\text{-H}_2\text{ase}$. While the system showed comparable activity under UV-visible irradiation due to efficient band gap excitation of TiO_2 (pathway 1), it showed significantly reduced activity under visible only irradiation at $\lambda > 420 \text{ nm}$ and displayed negligible H_2 yields at $\lambda > 455 \text{ nm}$ compared to $\text{CN}_x\text{-TiO}_2\text{-H}_2\text{ase}$ (Fig. S4†).⁹ Thus, UV-band gap excitation of TiO_2 dominates the absorption of the $\text{CN}_x\text{-TiO}_2\text{-H}_2\text{ase}$ hybrid material under UV-light irradiation, which becomes less significant under visible irradiation.

The effect of light intensity on the photocatalytic activity ($\lambda > 300 \text{ nm}$) was studied by employing neutral density filters. A photoactivity of approximately 90% remained when employing a 50% absorbance filter (50 mW cm^{-2}) and 44% of activity remained with an 80% filter (20 mW cm^{-2} ; Fig. S5†). The initial non-linear decrease in activity implies that the system is not limited by light at 1 Sun intensity as has been observed

previously with synthetic H_2 evolution catalyst-modified Ru dye-sensitised TiO_2 systems.¹⁸

The $\text{CN}_x\text{-TiO}_2\text{-H}_2\text{ase}$ system sets a new benchmark for visible light driven and prolonged H_2 production with a heterogenised H_2ase without the need for expensive or toxic materials.^{3,4,9} A part of this improvement can be attributed to the direct optical electron transfer (pathway 3) within $\text{CN}_x\text{-TiO}_2$, which draws the absorption of solar light significantly into the visible spectrum.

The enzyme loading onto $\text{CN}_x\text{-TiO}_2$ was calculated based on the BET surface area of $111 \text{ m}^2 \text{ g}^{-1}$, a crystallite surface area of $\sim 314 \text{ nm}^2$ per particle and an estimation that approximately one-quarter of the surface area of TiO_2 is accessible for the enzyme to adsorb. This equates to $\sim 0.1 \text{ H}_2\text{ase}$ per particle of $\text{CN}_x\text{-TiO}_2$. The approximate 1 : 10 enzyme : particle ratio allows the H_2ase to function at the maximum rate (*i.e.*, TOF) as the maximum electron flux of conduction band electrons is directed towards a single enzyme. To qualitatively determine the amounts of surface-bound and solubilised H_2ase in the optimised system, H_2ase (50 pmol) was loaded onto $\text{CN}_x\text{-TiO}_2$ (5 mg) in aqueous EDTA solution by stirring under N_2 for 15 min. The suspension was centrifuged and the supernatant decanted (see ESI† for experimental details). The $\text{CN}_x\text{-TiO}_2\text{-H}_2\text{ase}$ pellet was re-dispersed in fresh EDTA solution (3 mL, 0.1 M, pH 6) and the photocatalytic vessel purged with 2% CH_4 in N_2 . The suspension was then irradiated ($\lambda > 420 \text{ nm}$) and H_2 production monitored (Fig. 3). The H_2 production activity was nearly identical to a sample that was not centrifuged, both in the presence and absence of methyl viologen (MV^{2+} , see below), indicating that attachment of H_2ase to $\text{CN}_x\text{-TiO}_2$ is essentially quantitative. The substantially improved adsorption of the enzyme on the TiO_2 surface compared to the inert CN_x polymer therefore also contributes to the increased activity of $\text{CN}_x\text{-TiO}_2\text{-H}_2\text{ase}$ compared to $\text{CN}_x\text{-H}_2\text{ase}$. Previously an 88% decrease in photoactivity was observed with the poorly interacting CN_x -

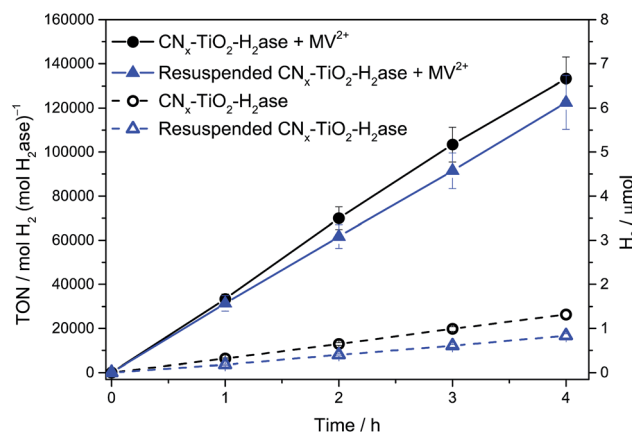


Fig. 3 Photocatalytic H_2 production using $\text{Dmb} \text{ [NiFeSe]-H}_2\text{ase}$ (50 pmol) in EDTA (pH 6, 0.1 M, 3 mL) with $\text{CN}_x\text{-TiO}_2$ (5 mg) under optimised conditions before and after centrifugation and re-suspension in fresh EDTA buffer solution followed by 1 Sun irradiation ($\lambda > 420 \text{ nm}$). Results are also shown in the presence and absence of redox mediator, methyl viologen (MV^{2+}).



H_2ase after centrifugation and re-dispersion in fresh electron donor buffer.⁹

The external quantum efficiency (EQE) of the $\text{CN}_x\text{-TiO}_2\text{-H}_2\text{ase}$ system was measured by applying narrow band pass filters ($\lambda = 360 \pm 10 \text{ nm}$; $I = 2.49 \text{ mW cm}^{-2}$ and $400 \pm 10 \text{ nm}$; $I = 4.34 \text{ mW cm}^{-2}$; see ESI† for experimental details). UV-irradiation gave an EQE of approximately 4.8% and under visible irradiation an EQE of 0.51% was obtained. These values are more than a 10-fold improvement over the UV and visible EQE for the $\text{CN}_x\text{-H}_2\text{ase}$ system,⁹ which can be attributed to the improved light absorption (Fig. S6†) and increased electron transfer rate due to adsorption of the H_2ase onto the particle surface.

We previously showed that a significantly increased photoactivity was observed under standard conditions using $\text{CN}_x\text{-H}_2\text{ase}$ upon addition of an excess of the redox mediator MV^{2+} , producing up to $77 \mu\text{mol H}_2$ after 69 h of UV-visible irradiation.⁹ A long-term experiment with H_2ase (50 pmol), $\text{CN}_x\text{-TiO}_2$ (5 mg) and added MV^{2+} (5 μmol) in aqueous EDTA (0.1 M) at pH 6 was performed with both $\lambda > 300 \text{ nm}$ light and with visible light only ($\lambda > 420 \text{ nm}$). Under UV-visible irradiation after 72 h, the $\text{CN}_x\text{-TiO}_2\text{-MV-H}_2\text{ase}$ system produced $193 \mu\text{mol H}_2$ with a $\text{TON}_{\text{H}_2\text{ase}}$ of $> 3.8 \times 10^6$ and an initial $\text{TOF}_{\text{H}_2\text{ase}}$ of 35 s^{-1} (Fig. S7†). Under visible-light only, $66 \mu\text{mol H}_2$ was produced with a $\text{TON}_{\text{H}_2\text{ase}}$ of 1.3×10^6 and an initial $\text{TOF}_{\text{H}_2\text{ase}}$ of 9 s^{-1} (Fig. S8†). The ratio of the amount of hydrogen produced in the presence and absence of MV^{2+} can be used to estimate the relative efficiency of the charge transfer from material to H_2ase . Under full spectrum irradiation ($\lambda > 300 \text{ nm}$) with $\text{CN}_x\text{-H}_2\text{ase}$ the ratio was found to be 22, whereas for both $\text{TiO}_2\text{-H}_2\text{ase}$ and $\text{CN}_x\text{-TiO}_2\text{-H}_2\text{ase}$ systems the ratio was 5. This strongly supports the fact that there is a significant improvement in the charge transfer from a TiO_2 -based material to H_2ase . In addition, this ratio remains constant when the wavelength of light used is restricted to the visible region ($\lambda > 420 \text{ nm}$).

The H_2 production rates in the presence of MV^{2+} are significantly higher than those obtained in the absence of MV^{2+} . The blue colour of the vials containing MV^{2+} is indicative of the formation of reduced MV^{+} in solution (Fig. S9†). By comparison, addition of MV^{2+} to the previously reported Ru-dye-sensitised $\text{TiO}_2\text{-H}_2\text{ase}$ system caused a slight decrease in activity, which was attributed to the decreased availability of electrons for the H_2ase and the absorption of incident photons by MV^{+} .^{3a} Here, solubilised MV^{+} does not limit light absorption by $\text{CN}_x\text{-TiO}_2$ significantly and is able to efficiently donate electrons to surface-bound H_2ase , resulting in increased H_2 production. This result implies that interfacial electron transfer from $\text{CN}_x\text{-TiO}_2$ to H_2ase is still not fully optimised in this system, where the orientation of the H_2ase is not fully 'directed'. Ideally, the distance from the $\text{CN}_x\text{-TiO}_2$ surface to the $[\text{Fe}_4\text{S}_4]$ electron transport chain should be minimised and an improved orientation of the enzyme would allow trapping of CB_{TiO_2} electrons more efficiently for maximised turnover.¹⁹

Favourable electron transfer kinetics at the $\text{CN}_x\text{-TiO}_2\text{-H}_2\text{ase}$ interface can be assumed based on previous reports. Electron transfer in the order of 10^7 s^{-1} was reported from CdS nanorods to an $[\text{FeFe}]\text{-H}_2\text{ase}$ isolated from *Clostridium*

acetobutylicum.^{4c} In addition, a long lived photo-excited state lifetime of $\tau_{1/2} \sim 0.8 \text{ s}$ was previously reported for TiO_2 conduction band electrons in a photocatalytic system with Ru dye-sensitised TiO_2 and electron transfer to co-immobilised molecular cobaloxime catalysts occurred with $\tau_{1/2} \sim 5$ to $50 \mu\text{s}$.²⁰ Based on these reports, we can assume that a reasonably long-lived TiO_2 conduction band electron is generated and that H_2ase is capable of readily collecting these electrons.

Conclusions

In summary, solar light driven H_2 production with a semi-biological system consisting of TiO_2 modified with polymeric CN_x and immobilised H_2ase has been demonstrated. We have shown that by improving the surface interaction of the enzyme with the light harvesting CN_x material, specifically by adsorption of the enzyme onto the TiO_2 surface, H_2 generation is drastically improved. Another important factor is the improved visible light absorption by direct CN_x excitation (pathway 2) and $\text{CN}_x\text{-TiO}_2$ charge transfer (pathway 3), which enables high photoactivity. The $\text{CN}_x\text{-TiO}_2\text{-H}_2\text{ase}$ assembly achieved a TOF of 8 s^{-1} and TON of $> 5.8 \times 10^5$ after 72 h in the absence of an external soluble redox mediator, thereby setting a new benchmark for photochemical architectures based on abundant and non-toxic materials and a heterogenised H_2ase . The additional use of the redox mediator MV^{2+} allowed for the photo-generation of H_2 with a TOF of 35 s^{-1} and a TON of $> 3.8 \times 10^6$. This work advances the use of hybrid photocatalytic schemes by integrating highly active electrocatalysts with advanced light absorbing materials such as $\text{CN}_x\text{-TiO}_2$, which is shown to be compatible with H_2ases in aqueous solution.

Acknowledgements

We acknowledge support by the Christian Doppler Research Association (Austrian Federal Ministry of Science, Research and Economy and National Foundation for Research, Technology and Development), the OMV Group and a Marie Curie fellowship to C.C. (GAN 624997624997). R.B. and L.W. acknowledge financial support by the MIWFT-NRW within the project "Anorganische Nanomaterialien für Anwendungen in der Photokatalyse". We thank Dr J. C. Fontecilla-Camps and Dr C. Cavazza (CNRS Grenoble, France) for providing us with *Dmb* [NiFeSe] hydrogenase, Ms Marielle Bauzan (CNRS Marseilles, France) for growing the bacteria, and Dr Michal Bledowski for assistance with $\text{CN}_x\text{-TiO}_2$ synthesis.

Notes and references

- (a) E. Reisner, *Eur. J. Inorg. Chem.*, 2011, 1005–1016; (b) P. W. King, *Biochim. Biophys. Acta*, 2013, **1827**, 949–957.
- (a) F. A. Armstrong, N. A. Belsey, J. A. Cracknell, G. Goldet, A. Parkin, E. Reisner, K. A. Vincent and A. F. Wait, *Chem. Soc. Rev.*, 2009, **38**, 36–51; (b) A. K. Jones, E. Sillery, S. P. J. Albracht and F. A. Armstrong, *Chem. Commun.*, 2002, 866–867; (c) W. Lubitz, H. Ogata, O. Rüdiger and E. Reijerse, *Chem. Rev.*, 2014, **114**, 4081–4148.



3 (a) E. Reisner, D. J. Powell, C. Cavazza, J. C. Fontecilla-Camps and F. A. Armstrong, *J. Am. Chem. Soc.*, 2009, **131**, 18457–18466; (b) E. Reisner, J. C. Fontecilla-Camps and F. A. Armstrong, *Chem. Commun.*, 2009, 550–552.

4 (a) B. L. Greene, C. A. Joseph, M. J. Maroney and R. B. Dyer, *J. Am. Chem. Soc.*, 2012, **134**, 11108–11111; (b) A. Bachmeier, V. C. C. Wang, T. W. Woolerton, S. Bell, J. C. Fontecilla-Camps, M. Can, S. W. Ragsdale, Y. S. Chaudhary and F. A. Armstrong, *J. Am. Chem. Soc.*, 2013, **135**, 15026–15032; (c) M. B. Wilker, K. E. Shinopoulos, K. A. Brown, D. W. Mulder, P. W. King and G. Dukovic, *J. Am. Chem. Soc.*, 2014, **136**, 4316–4324.

5 (a) C. E. Lubner, R. Grimme, D. A. Bryant and J. H. Golbeck, *Biochemistry*, 2010, **49**, 404–414; (b) H. Krassen, A. Schwarze, B. Friedrich, K. Ataka, O. Lenz and J. Heberle, *ACS Nano*, 2009, **3**, 4055–4061; (c) M. Ihara, H. Nishihara, K.-S. Yoon, O. Lenz, B. Friedrich, H. Nakamoto, K. Kojima, D. Honma, T. Kamachi and I. Okura, *Photochem. Photobiol.*, 2006, **82**, 676–682.

6 T. Sakai, D. Mersch and E. Reisner, *Angew. Chem., Int. Ed.*, 2013, **52**, 12313–12316.

7 (a) I. Okura, *Coord. Chem. Rev.*, 1985, **68**, 53–99; (b) O. A. Zadvornyy, J. E. Lucon, R. Gerlach, N. A. Zorin, T. Douglas, T. E. Elgren and J. W. Peters, *J. Inorg. Biochem.*, 2012, **106**, 151–155.

8 (a) X. Wang, K. Maeda, A. Thomas, K. Takanabe, G. Xin, J. M. Carlsson, K. Domen and M. Antonietti, *Nat. Mater.*, 2009, **8**, 76–80; (b) D. J. Martin, P. J. T. Reardon, S. J. A. Moniz and J. Tang, *J. Am. Chem. Soc.*, 2014, **136**, 12568–12571; (c) M. K. Bhunia, K. Yamauchi and K. Takanabe, *Angew. Chem., Int. Ed.*, 2014, **53**, 11001–11005.

9 C. A. Caputo, M. A. Gross, V. W. Lau, C. Cavazza, B. V. Lotsch and E. Reisner, *Angew. Chem., Int. Ed.*, 2014, **53**, 11538–11542.

10 (a) R. Beranek and H. Kisch, *Photochem. Photobiol. Sci.*, 2008, **7**, 40–48; (b) D. Mitoraj and H. Kisch, *Angew. Chem., Int. Ed.*, 2008, **47**, 9975–9978.

11 (a) A. Fujishima and K. Honda, *Nature*, 1972, **238**, 37–38; (b) M. Grätzel, *Nature*, 2001, **414**, 338–344; (c) Y. Ma, X. Wang, Y. Jia, X. Chen, H. Han and C. Li, *Chem. Rev.*, 2014, **114**, 9987–10043.

12 M. Bledowski, L. Wang, A. Ramakrishnan, O. V. Khavryuchenko, V. D. Khavryuchenko, P. C. Ricci, J. Strunk, T. Cremer, C. Kolbeck and R. Beranek, *Phys. Chem. Chem. Phys.*, 2011, **13**, 21511–21519.

13 M. Bledowski, L. Wang, A. Ramakrishnan, A. Bétard, O. V. Khavryuchenko and R. Beranek, *ChemPhysChem*, 2012, **13**, 3018–3024.

14 (a) E. Garcin, X. Verner, E. C. Hatchikian, A. Volbeda, M. Frey and J. C. Fontecilla-Camps, *Structure*, 1999, **7**, 557–566; (b) A. Parkin, G. Goldet, C. Cavazza, J. C. Fontecilla-Camps and F. A. Armstrong, *J. Am. Chem. Soc.*, 2008, **130**, 13410–13416; (c) C. S. A. Baltazar, M. C. Marques, C. M. Soares, A. M. DeLacey, I. A. C. Pereira and P. M. Matias, *Eur. J. Inorg. Chem.*, 2011, 948–962.

15 (a) M. C. Marques, R. Coelho, A. L. De Lacey, I. A. C. Pereira and P. M. Matias, *J. Mol. Biol.*, 2010, **396**, 893–907; (b) A. Volbeda, P. Amara, M. Iannello, A. L. De Lacey, C. Cavazza and J. C. Fontecilla-Camps, *Chem. Commun.*, 2013, **49**, 7061–7063.

16 (a) L. Wang, M. Bledowski, A. Ramakrishnan, D. König, A. Ludwig and R. Beranek, *J. Electrochem. Soc.*, 2012, **159**, H616–H622; (b) M. Bledowski, L. Wang, S. Neubert, D. Mitoraj and R. Beranek, *J. Phys. Chem. C*, 2014, **118**, 18951–18961.

17 K. Sayama and H. Arakawa, *J. Phys. Chem.*, 1993, **97**, 531–533.

18 F. Lakadamyali, M. Kato and E. Reisner, *Faraday Discuss.*, 2012, **155**, 191–205.

19 A. Bachmeier and F. Armstrong, *Curr. Opin. Chem. Biol.*, 2015, **25**, 141–151.

20 (a) F. Lakadamyali, A. Reynal, M. Kato, J. R. Durrant and E. Reisner, *Chem.-Eur. J.*, 2012, **18**, 15464–15475; (b) A. Reynal, J. Willkomm, N. M. Muresan, F. Lakadamyali, M. Planells, E. Reisner and J. R. Durrant, *Chem. Commun.*, 2014, **50**, 12768–12771.

